ORIGINAL RESEARCH ARTICLE

Study on synthesis and adsorption property of porous carbon/Ni nanoparticle composites

Sailu Xu[1], Yuxin Du[1], Meiqi Hui[1], Zichen Wang[1], Junfeng Zhao[1,2]*, Gang Yang[1,2]

[1] *School of Materials Engineering, Changshu Institute of Technology, Changshu 215500, Jiangsu Province, China. E-mail: jfzhao@cslg.edu.cn*

[2] *Suzhou Key Laboratory of Functional Ceramic Materials, Changshu 215500, Jiangsu Province, China*

Abstract

The porous carbon/Ni nanoparticle composite was prepared by a freeze-drying method using NaCl as the template. It was applied in the effect of the concentration, adsorption time, and temperature of adsorption on the adsorption behavior. The kinetic model and the adsorption isothermic fitting results show that the adsorption behavior fits with the pseudo-secondary dynamics and the Langmuir isothermal model, indicating that the adsorption process is monolayer adsorption. Thermodynamic results indicate that the adsorption process is spontaneous physicochemical adsorption. The fitting showed that the porous carbon/Ni nanoparticle composites reach 217.17 mg·g^{-1}, at 313 K indicates good adsorption for Congo red.

Keywords: Porous Carbon; Magnetic; Congored; Adsorption Performance

1. Introduction

With the steady development of the economy and the deepening of industrialization, dye wastewater has become an urgent pollution problem[1]. The adsorption method is simple and highly efficient. Porous carbon material (porous carbon material) is a porous material with carbon as the main body, which has the advantages of large than surface area, developed pores, good chemical stability, and a wide source of raw materials, rich resources, low price, and simple production process, which can carry out large-scale production. Therefore, it is widely used in energy storage and conversion, catalytic and macromolecular adsorption, and is favored by researchers at home and abroad[2,3]. According to the internationally recognized definition, porous carbon can be divided into three types: microporous carbon material (< 2 nm), iterporous carbon material (between 2–50 nm), porous carbon material (> 50 nm). In recent years, research has found that a single type of hole structure material cannot meet the market demand of high performance and high efficiency. Therefore, artificial transformation and design of porous carbon according to performance and application requirements has become a hot research topic, and the development and application of multiporous carbon materials have emerged[4,5]. In terms of sewage treatment, although porous carbon has the advantages of large than surface area and good adsorption performance when porous carbon is added to sewage for adsorption, it will be dispersed in water and cannot be

recycled, which leads to waste of resources and cost increase.

In this paper, porous carbon/Ni nanoparticle complexes were prepared by the freeze-drying method, using water-soluble inorganic salt NaCl as a template. The effect of adsorbent dosage, adsorption time, and temperature on the adsorption properties of porous carbon/Ni nanoparticle composites was investigated respectively, and the adsorption behavior of porous carbon/Ni nanoparticle composite is analyzed using kinetic and isothermic models.

2. Experiment

2.1 Preparation of porous carbon/Ni nanoparticle composites

0.003 mol $Ni(NO_3)_2 \cdot 6H_2O$ and 4 g NaCl, were dissolved in 20 mL deionized water, quantity 10 mL egg white was added to the above solution, stirred with a magnetic mixer for 30 min, and mixing evenly for standby. The mixture liquid is frozen in liquid nitrogen for 10 min to completely frozen, and the vacuum sublimation treatment for 48 h is removed to completely sublimate the water. Frozen dried samples were removed and placed into the crucible. The heat-treated samples were removed at 650 ℃ for 3 h. In N_2 atmosphere, ground dispersed in a certain amount of deionized water, the NaCl template was sonicated, and the samples were then extracted and separated, repeated to fully remove inorganic salt 3 times. The aspirated/Ni nanoparticle-washed samples were prepared by drying in a 60 ℃ vacuum drying tank for 8 h, to obtain a porous carbon/Ni nanoparticle composite.

2.2 Characterization of the material topography and structure

The structure was analyzed by the X-ray diffraction instrument (XRD), the scanning electron microscopy (SEM, SIGMA, 20 kV) and high-resolution transmission electron microscopy (HRTEM, JEOL-2000 CX, 200 kV), and the specific surface area and aperture size analyzer (BET) were used to analyze the specific surface area and pore structure.

2.2 Characterization of the adsorption properties

The sorbent properties of porous carbon/Ni nanoparticle composites were determined using a TU-1901 UV spectrophotometer. The adsorption properties of the adsorbent were studied, using Congo Red (CR) as a pollutant model, at 20, 40, 60, 80, 100 mg/L concentrations. A solution of CR at 40 mg/L and investigated the effects of different temperatures (298, 303, 308, 313 K) on the adsorption properties. All the above experiments were performed at 200 r·min^{-1} oscillations, with 5 mL mixed solution at 15 min, 30 min, 1 h, 2 h, 3 h, placed into a centrifuge tube, centrifugation for 5 min, and the remaining CR concentration was tested using a UV spectrophotometer.

3. Results and discussions

Figure 1 shows the XRD map of the prepared porous carbon/Ni nanoparticle composite, showing three sharp diffraction peaks at 2θ at 42.2°, at 51.9° and 76.2°, corresponding to (111), (200), (220) crystal surface diffraction of Ni (PDF#65-0380), respectively. Furthermore, a bulging, relatively weak diffraction peak was observed at 2θ of 25.6°, analyzed corresponding to the characteristic diffraction peak of amorphous carbon. No other miscellaneous peaks were observed, indicating that there was no impurity phase in the composite product. XRD results show that the products prepared by freeze drying-carbonization are C/Ni composite, the carbon component in protein converted to carbon material by high temperature thermolysis; nickel nitrate generates nickel oxide by high temperature, the temperature increases further, nickel oxide by carbon reduction generates magnetic nanoparticle, and eventually form porous carbon/magnetic Ni nanoparticle composite material.
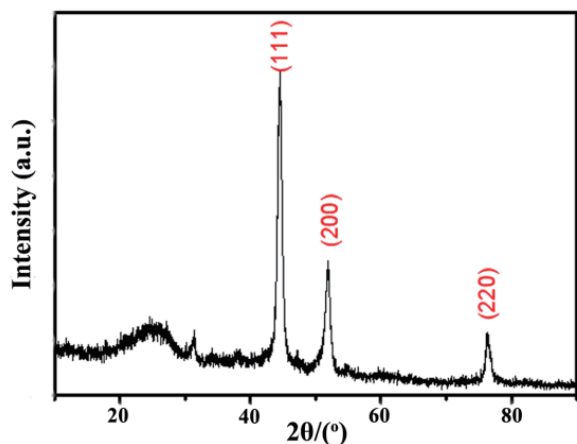
Figure 1. XRD plot of the porous carbon/Ni nanoparticle composites.

(a) 5,000 times;   (b) 20,000 times
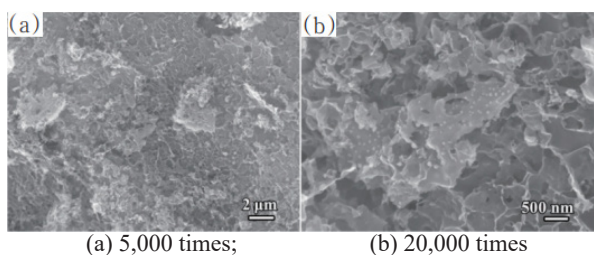
Figure 2. XRD diagram of porous carbon /Ni nanoparticle composites.

As can be seen from **Figure 2**, the material prepared by freeze-drying-carbonization presents a 3D structure similar to the block material of "frozen tofu". Further observation found that the surface of 3D carbon material presents irregular sheet structure, in layer by layer pit gully successively filled with holes from large to small. It is believed that during the reaction precursor of liquid nitrogen freezing, NaCl cubic crystal and nickel nitrate crystal precipitate out rapidly with the sharp drop of temperature, and a large number of NaCl cubic crystal particles are self-stacked to form a 3D structure. Nickel nitrate crystals are distributed in the 3D structure, and the proteins in the precursor are also precipitated with decreasing temperature and coated in the surface of the NaCl cubic crystals. Further vacuum sublimation drying completely removes the water from the system, thus forming a protein/nickel nitrate/NaCl composite powder product. Complex powder at high temperature in an inert atmosphere, NaCl structure remains stable at high temperature, the protein carbonization on the surface is transformed into carbon material, and nickel nitrate forms nanoparticles by decomposition and reduction reaction and nanoparticles. The product, removed from the NaCl template with simple washing, forming a honeycomb porous carbon structure with more evenly distributed dimensions, interconnected and interconnected.

Figure 3(a)–**Figure 3(c)** is a TEM plot of porous carbon/Ni nanoparticle complexes. It can be seen that the sample has a 3D structure of which the matrix is the porous carbon. The porous carbon structure is filled with high-density, ultra-fine nickel nanoparticles with a size of approximately 30 nm. The HRTEM plot of **Figure 3(d)** shows a distinct crystal surface orientation in the local region, corresponding to the crystal surface spacing of Ni in the composite, covered with helminth-like disordered ripples of the nickel, corresponding to the amorphous carbon layer. This result is consistent with the XRD results, indicating that nanoparticles distributed in graded porous carbon form a composite structure.
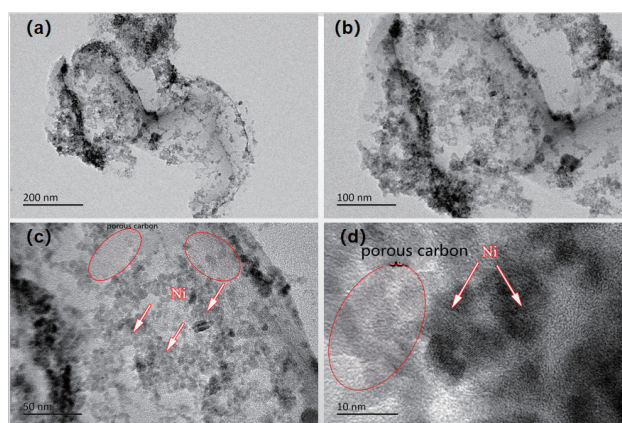
Figure 3. (a) (b) (c) TEM figures of multiwell carbon/Ni nanoparticle composites and **(d)** HRTEM figure.

According to the BET adsorption/desorption of **Figure 4(a)** porous carbon/Ni nanoparticle composite, the sample presents a I/IV mixed adsorption model indicating the presence of a hierarchical porous structure of the material. First, the significant uptrend at $P/P_0 < 0.01$ was attributed to type I isotherms, indicating the presence of a micropore structure in the structure. At $P/P_0 = 0.4$–0.9, there is a distinct suction attachment hysteresis loop in the relative pressure range, in line with the IV isothermic model, showing a large number of interpore structures in the structure. Besides, when $P/P_0 > 0.9$, the adsorption/desorption is further increased,

indicating that large pore structures still exist in the structure[6–7]. Therefore, the material prepared in this experiment is a graded porous structure. The analysis of Brunauer-Emmett-Teller (BET) showed that the specific surface area of porous carbon/Ni nanoparticle composites is up to 511.532 $m^2 \cdot g^{-1}$. The aperture distribution curves of the sample are further given in **Figures 4(b)** and **4(c)**, and Barrett-Joyner-Halenda (BJH) and Dubinin Radushkevich (DR) analysis showed that the sample showed a distinct aperture distribution in both the 2–30 nm and the micropore region of 0–2 nm. By the observation, we know that the distribution of pore diameter is relatively concentrated, and the mesole mostly concentrated around 5 nm and the micropore around 0.3 nm, further proving that the sample has a better graded porous structure. Among them, the total adsorption pore volume was 0.938 $cm^3 \cdot g^{-1}$, BJH adsorption cumulative interpore and total pore volume were 0.859 $cm^3 \cdot g^{-1}$,

DR method micropore (< 2 nm) volume was 0.236 $cm^3 \cdot g^{-1}$.

Figure 5 shows plots of the adsorption properties of Congo red dye in porous carbon/Ni nanoparticle composites at 298, 303, 308, 313 K. As can be seen from the figure, the adsorption curve rises sharply when the adsorption time is within 60 min, and then tends to be flat. It shows that the adsorption tends to achieve saturation at 60 min. The intercepted 60 min time point and the adsorption concentration are 40 $mg \cdot L^{-1}$ (in the order of temperature rise), respectively, are 105.37, 124.37, 158.52, 163.87 $mg \cdot g^{-1}$, indicating that the adsorption amount will increase as the temperature increases (the increase rate is gradually slowed and reaches saturation at a temperature). It shows that as the temperature increases, the concentration of the adsorption matter will also affect the size of the adsorption quantity.
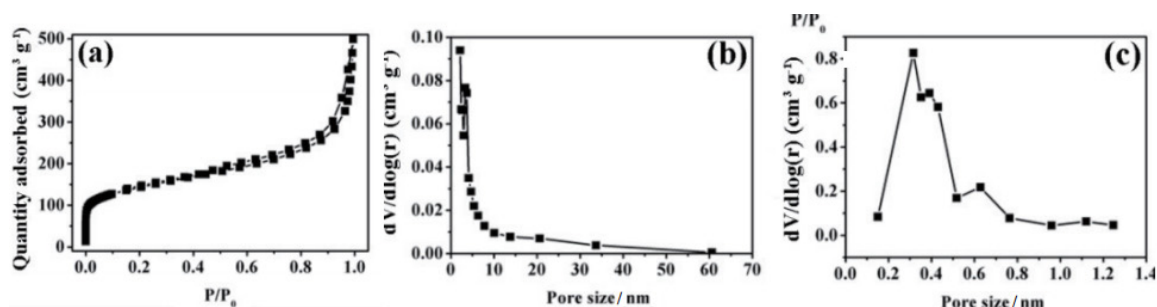
Figure 4. Diagram of BET and aperture distribution of Porous carbon/Ni nanoparticle composites. **(a)** BET adsorption/detachment map; **(b)** distribution map of interpore aperture map; **(c)** micropore aperture distribution map.
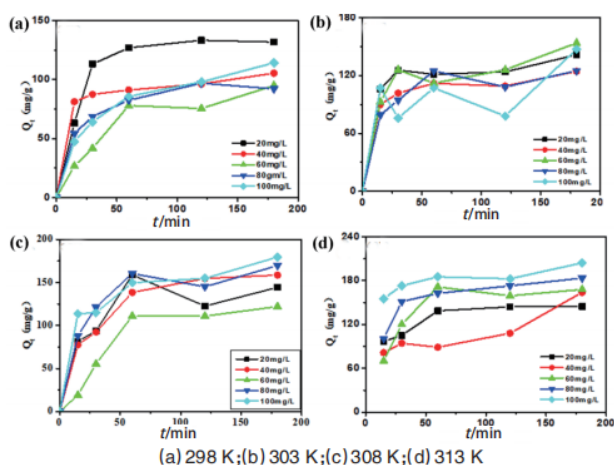
Figure 5. Effects of different temperatures on the adsorption properties.

To further explore the adsorption behavior of

porous carbon/Ni nanoparticle composites on the organic dye Congo red, a pseudo-second-order kinetic model was used to fit the adsorption data at different temperatures, with the exact formula shown in equation (1)[8].

$$\frac{t}{q_t} = \frac{1}{k_2 q_e^2} + \frac{t}{q_e} \tag{1}$$

The q_e, q_t ($mg \cdot g^{-1}$) represent the adsorption capacity of t (min) at equilibrium and at some time, respectively; k_2 represents the pseudo-second-order rate constant ($g \cdot mg^{-1} \cdot min^{-1}$).

Figures 6(a)–**Figure 6(d)** shows a pseudo-fitting second-order nonlinear fitting curve for the adsorption behavior of porous carbon/Ni nanoparticle

Table 1. The fitting parameters of pseudo-second order dynamics of porous carbon/Ni nanoparticle composites to Congo red adsorption

Temprature /K	C_0/ (mg·L^{-1})	Parameters of Pseudo-kinetic model		
		k_2/ (g·mg^{-1}·min^{-1})	$q_{e, cal}$/ (mg·g^{-1})	R^2
	20	0.080 6	104.65	0.992 6
	40	0.074 3	107.41	0.994 7
298	60	0.414 7	117.10	0.950 1
	80	0.122 2	117.70	0.994 2
	100	0.231 6	119.53	0.991 1
	20	0.086 2	147.06	0.986 1
	40	0.064 9	125.79	0.989 6
303	60	0.096 7	159.74	0.965 5
	80	0.071 4	127.23	0.982 7
	100	0.153 4	150.60	0.901 3
	20	0.079 9	149.48	0.964 5
	40	0.121 6	179.53	0.994 9
308	60	0.010 0	176.06	0.997 7
	80	0.079 4	177.30	0.988 0
	100	0.085 9	189.04	0.985 9
	20	0.063 2	153.85	0.997 6
	40	0.203 3	170.94	0.824 7
313	60	0.089 6	184.84	0.984 9
	80	0.060 7	193.80	0.998 2
	100	0.033 4	206.19	0.992 3

complexes at 298, 303, 308, 313 K temperatures. The kinetic parameters (k_2 and q_e) and regression coefficients (R^2) of the fitted model are shown in **Table 1.** For all four adsorption temperatures, the experimental data agree with the regression coefficients (R^2 substantially above 0.99) at all initial concentrations. From these R² values, the model of quasi-second order is suitable to describe the adsorption kinetic behavior. The pseudo-second-order model calculations agree well with the experimental observations. These results confirm that chemical adsorption is a rate control step and depends on the concentration of contaminants exposed to the surface of the porous carbon/Ni nanoparticle composite materials[9]. Furthermore, the maximum adsorption of the Congo red dye at 100 mg·L^{-1} by the porous carbon/Ni nanoparticle composite at 298, 303, 308, 313 K was 119.53, 150.60, 189.04, and 206.19 mg·g^{-1}, respectively.

The interaction of adsorbent with adsorbate describes as adsorption isotherms. The well-known model Langmuir isotherm describes the adsorption process.
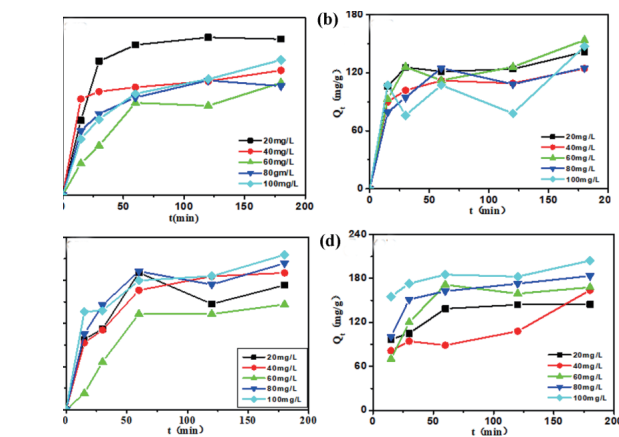
Figure 6. Fof pseudo-second-order dynamics of the adsorption process.

Langmuir isotherms are based on single-molecule adsorption processes, commonly used to describe equilibrium adsorption isotherms on homogeneous surfaces. The isothermal model can represent as Equation (2)[10,11].

$$q_e = \frac{q_m K_L C_e}{1 + K_L C_e} \tag{2}$$

C_e is the equilibrium concentration of the solute (mg·L^{-1}); q_e indicates the adsorption amount

(mg·g^{-1}) at equilibrium; q_m is the maximum adsorption amount (mg·g^{-1}); and K_L indicates the Langmuir adsorption constant (g^{-1}). **Figure 7** shows the fit diagram of the Langmuir isothermal model. The relevant parameters obtained from the isothermal model fitting listed in **Table 2** show that the regression coefficient R^2 is above 0.9 at different adsorption temperatures, saying that the bright Muir model can well describe the adsorption behavior of porous carbon/Ni nanoparticle composite adsorption agent. The isothermal fitting showed that the porous carbon/Ni nanoparticle composite is monolayer adsorption, and the adsorption is in a monolayer. Once the adsorption cannot be further at that position once the dye molecule occupies the active site on the magnetic porous carbon surface[12]. By the fitting calculation, we can get that the maximum adsorption of Congo red by the porous carbon/Ni nanoparticle composite was 123.10, 144.95, 197.53, and 217.17 mg·g^{-1}. at 298, 303, 308, 313 K, respectively.
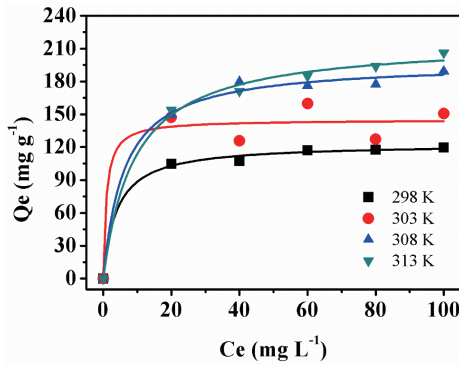
Figure 7. A fitting of the Langmuir isothermic model for the adsorption process.

Table 2. Langmuir fitting parameters for the isotherm model

T /K	Langmuir		
	q_m/ (mg^{-1}·g^{-1})	K_L/ (L·mg^{-1}) $\times 10^3$	R^2
298	123.10	0.254 9	0.996 7
303	144.95	0.111 1	0.948 1
308	197.53	0.163 1	0.995 1
313	217.17	0.110 4	0.994 7

To further evaluate the effect of temperature on the adsorption properties of porous carbon/Ni nanoparticles composites, thermodynamic parameters, including enthalpy (ΔH^o), Gibbs free energy (ΔG^o), and entropy (ΔS^o) were calculated, with the specific equations of:

$$\Delta G^o = -RT \ln K \qquad (3)$$

$$\ln K = \frac{-\Delta H^o}{RT} + \frac{\Delta S^o}{R} \qquad (4)$$

R is the gas constant (8.314 J·mol^{-1}·K^{-1}), T indicates the temperature (K), and K is the adsorption equilibrium constant. **Figure 8** shows a linear plot of ln$K$ and 1/T. The specific values of the thermodynamic parameter enthalpy (ΔH^o), Gibbs free energy (ΔG^o), and entropy (ΔS^o) are calculated by fitting shown in **Table 3**.
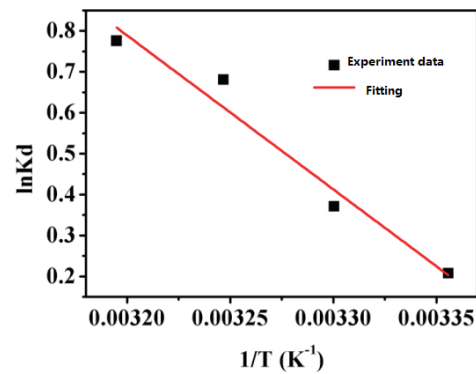
Figure 8. Linear plot between ln$K$ and 1/T.

Table 3. Specific values for the enthalpy of thermodynamic parameters (ΔH^o), Gibbs free energy (ΔG^o), and entropy (ΔS^o)

T/K	ΔG^o/ (kJ·mol^{-1})	ΔH^o/ (kJ·mol^{-1})	ΔS^o/ (kJ·mol^{-1}·K^{-1})
298	−0.51		
303	−0.94		
308	−1.74	31.25	0.11
313	−2.02		

From **Table 3**, all of the ΔG^o value is negative, indicating that the Congo red adsorption of the porous carbon/Ni nanoparticle composite is a spontaneous process. The ΔG^o tends to decrease with the increasing temperature, which indicates that the increased temperature is favorable for adsorption. ΔH^o and ΔS^o are all positive, which indicates that the adsorption of porous carbon/Ni nanoparticle composite to Congo red has exothermal properties[13]. ΔH^o is 31.25 kJ·mol^{-1}, higher than physical adsorption heat (2.1–20.9 kJ·mol^{-1}) and less than chemical adsorption heat (80–200 kJ·mol^{-1}), indicating that the adsorption of porous carbon/Ni nanoparticle composite belongs to a physicochemical adsorption process[14].

4. Conclusion

The porous carbon/Ni nanoparticle composites synthesized by a freeze-drying method by NaCl as a template. SEM and TEM showed that Ni nanoparticles equably distributed on porous carbon carriers, which constructed into a 3D-graded porous structure. The BET and pore size distribution results show that the porous carbon/Ni nanoparticle composite is a graded porous structure composed of large holes, mesholes and micropores, with 511.532 $m^2 \cdot g^{-1}$ and 0.938 $cm^3 \cdot g^{-1}$. Compared to the surface area and the total adsorption pore volume, respectively, making the porous carbon/Ni nanoparticle composite has excellent adsorption properties. The kinetic and thermodynamic results show that the adsorption behavior, which is the composite materials to the organic pollutant Congo red, accords with the pseudo-secondary dynamics and Langmuir isothermal model. And it is with a maximum adsorption amount of 217.17 $mg \cdot g^{-1}$ at 313 K.

Conflict of interest

The authors declare that they have no conflict of interest.

References

1. Lu Y, Song S, Wang R, *et al.* Impacts of soil and water pollution on food safety and health risks in China. Environment International 2015; 77: 5–15.

2. Chen B, Ma Q, Tan C, *et al.* Carbon-based sorbents with three-dimensional architectures for water remediation. Small 2015; 11(27): 3319–3316.

3. De S, Balu AM, Van Der Wall JC, *et al.* Biomass-derived porous carbon materials: synthesis and catalytic applications. ChemcatChem 2015; 7(11): 1608–1629.

4. Sevilla M, Ferrero GA, Fuertes AB. One-pot synthesis of biomass-based hierarchical porous carbons with a large porosity development. Chemistry of Materials 2017; 29(16): 6900–6907.

5. Liu R, Liu Y, Zhou X, *et al.* Biomass-derived highly porous functional carbon fabricated by using a free-standing template for efficient removal of methylene blue. Bioresource Technology 2014; 154: 138–147.

6. Gupta K, Gupta D, Khatri OP. Graphene-like porous carbon nanostructure from Bengal gram bean husk and its application for fast and efficient adsorption of organic dyes. Applied Surface Science 2019; 476: 647–657.

7. Song Y, Wei G, Kopec M, *et al.* Copolymer-templated synthesis of nitrogen-doped mesoporous carbons for enhanced adsorption of hexavalent chromium and uranium. ACS Applied Nano Materials 2018; 6(1): 2536–2543.

8. Ho YS, Mckay G. Pseudo-second order model for sorption processes. Process Biochemistry 1999; 34(5): 451–465.

9. Pour ZS, Ghaemy M. Removal of dyes and heavy metal ions from water by magnetic hydrogel beads based on poly (vinyl alcohol)/ carboxymethyl starch-gpoly (vinyl imidazole). RSC Advance 2015; 5: 64106–64118.

10. Hemmati F, Norouzbeigi R, Sarbisheh F, *et al.* Malachite green removal using modified sphagnum peat moss as a low-cost biosorbent: kinetic, equilibrium and thermodynamic studies. Journal Taiwan Institute of Chemical Engineers 2016; 58: 482–489.

11. Liu Y, Xu H. Equilibrium, thermodynamics and mechanisms of Ni^{2+} biosorption by aerobic granules. Biochemistry Engineering Journal 2007; (35): 174–182.

12. Cheng B, Le Y, Cai W, *et al.* Synthesis of hierarchical $Ni(OH)_2$, and NiO nanosheets and their adsorption kinetics and isotherms to Congo red in water. Journal of Hazardous Materials 2011; 185(2-3): 889–897.

13. Zhao J, Zha J, Yang C, *et al.* Cauliflower-like Ni/ NiO and NiO architectures transformed from nickel alkoxide and their excellent removal of Congo red and Cr(VI) ions from water. RSC Advance 2016; 6: 103585–103593.

14. Liu S, Ding Y, Li P, *et al.* Adsorption of the anionic dye Congo red from aqueous solution onto natural zeolites modified with N, N-dimethyl dehydroabietylamine oxide. Chemical Engineering Journal 2014; 248: 135-144.